OPEN ACCESS

Research

Journal of Oil, Gas and Petrochemical Sciences

Wellbore instability prediction and performance analysis using Poroelastic modeling

Dr. Ing Mohamed Halafawi,[1] Dr. Ing Lazăr Avram[2]

[1]Doctor and Inginer, Petroleum-Gas University of Ploiesti, Romania

[2]Professor; Drilling, Extraction, and Transportation of Hydrocarbons, Petroleum-Gas University of Ploiesti, Romania

Correspondence: Dr. Ing Mohamed Halafawi, Doctor and Inginer, Petroleum-Gas University of Ploiesti, Romania, Email: halafawi_2008@yahoo.com

Received: April 18, 2019 | **Published:** July 11, 2019

Abstract

Wellbore instability problems give rise to increasing the non-productive time (NPT) and the non-productive cost while drilling tectonically stressed and unstable formations. In this article, a wellbore stability model is developed for predicting the behavior of borehole instability zones and the optimum wellbore trajectory which has the safest mud window with time. Geo-Mechanical Earth Model (MEM) was combined with failure criterion using logging while drilling /measurement while drilling (LWD/MWD) or wire line logging data as well. The developed model is generated iteratively in order to predict the optimum mud window and wellbore trajectory variations with time. The radial and tangential stress concentrations around the wellbore are determined using the poroelastic constitutive model. This model enables to take into consideration the effect of the rock pore structure. Failure criteria considering the intermediate stress are also used as the shear failure criterion. Additionally, the model provides more precise solutions to optimize the drilling fluids in this high tectonic area. The model is applied and verified in a deviated wellRBS-91 in which exist excessive mechanical wellbore breakouts while drilling the 8.5" hole section. The developed model shows a good results in predicting the wellbore instability compared with the actual wellbore images for instability zones (3650 m – 3800 m). For a long time period (30 hrs) after drilling this zone, the developed model shows that the maximum shear stress around the wellbore is at 63º and 243º counterclockwise which agree with the image logs. The safe pressure window is very narrow at the high deviation angle at the current well azimuth (240º). The minimum and maximum safe mud weight in order to avoid shear and tensile failure are found 9.8 and 15.5 ppg respectively. This well section obviously cannot be drilled horizontally in direction of the minimum horizontal stress (Azimuth = 60º) due to the narrow allowable mud window.

Keywords: Wellbore stability models, failure criteria, instability prediction, safe mud weight, optimum well trajectory

Introduction

Borehole instability is described as an undesirable state of an open hole interval that does not maintain its gauge size and shape and/or its structural integrity. Instability causes are divided into three categories:[1-4] Mechanical (due to in-situ stresses), Erosion (due to fluid circulation), and Chemical (due to interaction of borehole fluid with the formation).Borehole instability gives rise to problems in drilling operations and design procedures. Instability problems produces non-productive time and sometimes also loss of equipment which means additional non-productive costs. Instability problems can appear in both vertical deviated and horizontal wells. Long extended reach deviated wells are especially known for having instability problems. Wells stability evaluation represents a rock mechanics problem which means prediction of a rock's response to mechanical loading.[1-3,5] Some special circumstances that make evaluation of stability problematic:[1-3,5]

- No methods available for direct observation of what is happening for the drill bit when it is several thousand of meters away
- Large variations in formation stresses and unsystematically in-situ stresses measurements.
- Large variations in the material properties of the formations and the limited amounts of material available for rock mechanics testing due to high-costed coring.
- Acting forces on the formation around the wellbore such as mud chemistry, redistribution of stresses, temperature changes, etc.

Numerous wellbore stability models have been developed since the past decades in order to tackle wellbore instability problems and determine a safe mud window, however, these models have a number of shortcomings. Most of the published models have assumptions of an elastic rock material, material, a time-independent of borehole failure and no effect of the intermediate stress on the rock strength.

Recently, the models that consider the fully coupled poroelastic phenomenon require a lot of parameters, which may not available and time-consuming computation, such as the core data. Over the past decade, several contributions have been performed for the successful drilling of wells in the oil and gas industry. A wellbore stability analysis was carried out by Fuf et al.[6] before drilling the first horizontal well in the German Sector of the North Sea region. Eight vertical offset wells data in the area were analyzed and used to develop a MEM in order to simulate the horizontal wellbore design and trajectory behavior prior execution.

Ong and Roegiers,[7] suggested an anisotropic wellbore stability model in order to determine the stress around the well bore. The model led to deduce that the well bore collapse is affected by the degree of the rock strength in horizontal wellbore. They also found that pore pressure and Biot's constant affect the shear failure, however, their effect is

less obvious. Morita[8] presented a borehole trajectory study effect on wellbore stability. The study deduced that an oriented wells have a non-uniform stress distribution around the bore hole.

Hodge et al.[9] developed a time-dependent wellbore stability model by performing a fully coupled poroelastic model. In this model, the stress changes around well bore induced by the fluid flow are taken in consideration using finite element method. In order to analyze the stability of the borehole, the developed model is utilized in various formation types, stress regimes, and drilling circumstances.

Rabaa et al.[10] studied borehole instability for effective drilling and reservoir management determination. in order to minimize the risk of wellbore instabilities as wellbore breakouts for an extended reach horizontal hole, the study was used to identify the optimum mud weight and well azimuth. They deduced that the horizontal wells in the direction of the maximum principal horizontal stress is preferable in order to maximize the margin of the wellbore stability and to minimize the minimum required mud weight during drilling.

Li and Purdy[11] deduced two methods to estimate maximum horizontal stress. The first technique is based on the theory of equilibrium of three in-situ stresses components, the pore pressure, and the generalized Hooke's law. In this technique, a decrease in the uncertainty of in-situ stress is achieved. The second one includes the drilling breakouts and induced near-wellbore stresses analyses using the Mohr-Coulomb failure criterion.

Qi et al.[12] modeled the poroelasticity effect on wellbore stability for under balanced and overbalanced drilling conditions. An analytical coupled poroelastic modeling is studied for the over-balanced and underbalanced drilling scenarios. A time-dependent failure occurring inside the formation instead of at the wellbore wall is resulted.

Manshad et al.,[13] performed a wellbore stability analysis for vertical, deviated and horizontal wells utilizing analytical and numerical techniques. In this stability analysis, various rock failure criteria such as Mohr-Coulomb, Modified Lade, Mogi–Coulomb, and Tresca yield criterion are used for the optimum well trajectory and mud weight determinations. The predicted mud weight calculated using all these criteria is found giving reliable results. Nevertheless, Tresca and Mohr-Coulomb criteria are found overestimating the minimum required mud pressure to maintain the wellbore stability. Additionally, another wellbore stability models used for horizontal and deviated wells based on in-situ stresses equations are presented by Halafawi[14], Yi[15], and Mohiuddin[16]. The role of rock strength criteria in wellbore stability and trajectory optimization is presented by Chabook[17].

A good understanding of the preceded various chronological wellbore stability of the above models, their techniques and calculations is essential for selecting good practical instability prediction model for overcoming the resulting drilling instability wellbore problems. Additionally, since the rock is a porous medium, its mechanical response alters due to the fluid present inside the pores, and the limited data available, the poroelastic model with the same assumptions of previous authors will be assumed in order to take into account the phenomena of the interaction between the reservoir pressure and rock deformation, and to recommend a better practice for future operations.

Therefore, the main aim of this paper is to developed an integrated time-dependent well bore instability model in order to predict the wellbore stability issues in the pre-drilling stage and to simulate and analyze wells stability of RBS-91 field. Theory about borehole stability is presented for vertical and deviated wells with the different equations required for determining borehole fracturing and collapse. The developed model depends only on offset well-logs data and a less time-consuming mathematical descriptions so that the safest well path, as well as the optimum safe mud weight, can be determined. Additionally, the model is used to determine if this will as a candidate for underbalanced drilling or not.

Developed Wellbore Stability Model

To satisfy the objective of being able to run the developed model to predict wellbore instability problems anddetermine the optimum mud weight for future drilling activities, it is necessary to describe insitu stresses and pore pressure, circular wellbore stresses, cartesian stresses in three dimensions, rock failure criteria, rock mechanical properties and rock strength, and time-dependent wellbore stresses.

Insitu Stresses and Pore Pressure Prediction

The magnitude and orientation of in-situ stresses affect greatly the wellbore stability. The principal in-situ stresses are expressed as vertical stress (σ_v), minimum horizontal stress (σ_h) and maximum horizontal stress (σ_H). In order to predict wellbore stability, these stresses are used to develop the geomechanical earth model (GEM). Several authors have presented various equations to determine theinsitu stresses using different assumptions and techniques as follows:

Vertical in-situ stress

The vertical stress or overburden stress is the main principle stress which direction is directing to the earth's center. The magnitude of σ_v is estimated by the integration of rock densities at each incremental depth from surface to the depth of interest.[15,18] At any depth, The rock has various lithology and porosity, therefore the rock density varies. Rock density data is most commonly acquired LWD data.

$$\sigma_v = \int_0^H \rho_b(h)\,dh \quad (1)$$

Minimum horizontal stress

In order to determine the minimum horizontal stress, the only fully reliable method is to fracture the formation and find the fracture closure pressure, this test known as Micro frac and Extended Leak-off (XLOT) tests.[2] However, correlations and equations 2 through 6 shown in Table (1) also give a reasonable values.

Maximum horizontal stress

Maximum horizontal stress magnitude and orientation can be determined from the inversion of calibration of borehole failure such as breakouts, washouts, drilling-induced fractures and drilling problems.[15] However, several authors have presented various equations 7 through 10 which are appeared in Table (2) in order to a reasonable value for prediction modeling.

Pore Pressure Prediction

A formation pressure or pore pressure can be determined by kicks, resistivity logs, or sonic velocity logs but the most widely method to estimate the pore pressure is Eaton[29] as follows:

$$P_r = \sigma_v - (\sigma_v - P_{rn})\left(\frac{\Delta t_{norm}}{\Delta t_{\log}}\right)^x \quad (11)$$

Citation: Halafawi DIM, Avram DIL. Wellbore instability prediction and performance analysis using Poroelastic modeling. *J Oil Gas Petrochem Sci.* (2019);2(2):93-106. DOI: 10.30881/jogps.00028

Table 1. Minimum horizontal stress correlation and equations.

Author/PublisherName	Min. Horizontal Stress Formula	
Yi et al.[15],Hudson et al.[19], and Biot[20]	$\sigma_h = \frac{\upsilon}{1-\upsilon}\left(\sigma_v - \alpha_b P_p\right) + \alpha_b P_p$	(2)
Ahmed et al.[21], Cipolla et al.[22], and Iverson[23]	$\sigma_h = \frac{\upsilon}{1-\upsilon}\left(\sigma_v - \alpha_b P_p\right) + \alpha_b P_p + \sigma_{tec}$	(3)
Mike Mullen Equation[19]	$\sigma_h = \sigma_v\left(\frac{\nu_{fast}}{1-\nu_{fast}}\right) - \alpha P_r\left(1-\frac{\nu_{fast}}{1-\nu_{fast}}\right)$	(4)
Blanton and Olson[24]	$\sigma_h = \nu C_1 \varepsilon_{tec} + C_2$ Where $C_1 = \frac{E}{1-\nu^2}$ $C_2 = \frac{\nu\sigma_V + (1-2\nu)\alpha P_p + E\ \alpha\ t\ \Delta T}{1-\nu}$ $\varepsilon_{tec} = \frac{S_h - C'_2}{\nu C'_1}$	(5)
Harikrishnan and Hareland[25]	$\sigma_h = K_o\left(\sigma_v - \alpha P_p\right) + \alpha P_p$ Where $K_o = 1 - sin\beta$ $\beta = \arcsin\left(\frac{S_2 - S_1}{S_2 - S_1 + 4\Delta}\right)$ $S_1 = C_o\left(1 + a_s\left(P_e - \Delta\right)\right)^{b_s}$ $S_2 = C_o\left(1 + a_s\left(P_e + \Delta\right)\right)^{b_s}$	(6)

Table 2. Maximum horizontal stress correlation and equations.

Author/Publisher Name	Max. Horizontal Stress Formula	
Barton et al.[26]	$\sigma_H = \frac{C_o + \Delta P_w + 2P_r}{1-2\cos 2\theta} - \sigma_h \frac{1+2\cos 2\theta}{1-2cos\ \theta}$	(7)
Mike Mullen Equation[19]	$\sigma_H = \sigma_v\left(\frac{\nu_{slow}}{1-\nu_{slow}}\right) - \alpha P_r\left(1-\frac{\nu_{slow}}{1-\nu_{slow}}\right)$	(8)
	$\frac{\sigma_H}{\sigma_h} = \nu\left(1+\frac{1}{K_\beta}\right) + \frac{P_p}{\sigma_v}\left[1-\nu\left(1+\frac{1}{K_\beta}\right)\right]$	(9)
Addis et al.[27,28]	$\frac{\sigma_H}{\sigma_h} = \nu\left(1+K_\beta\right) + \frac{P_p}{\sigma_v}\left[1-\nu\left(1+K_\beta\right)\right]$ Where $K_\beta = \frac{\sin(\varnothing+2\beta)+\sin\varnothing}{\sin(\varnothing+2\beta)-sin\varnothing}$	(10)

Citation: Halafawi DIM,Avram DIL.Wellbore instability prediction and performance analysis using Poroelastic modeling. *J Oil Gas Petrochem Sci.* (2019);2(2):93-106. DOI: 10.30881/jogps.00028

Circular Wellbore Stresses

Before making a borehole, a rock is loaded on all sides and has uniform stresses in all directions. This case is then defined as in situ stress state. When a borehole is drilled in the center of the formation region, the stress state around the hole will vary due to the new geometrical element. This state around the hole is described as a stress concentration. The two stress categories resulted due to conditions modifications are in-situ/rock stresses and stresses around the hole. The Kirsch equations[2,3,30] and their derivatives are the most important equations related to applied rock mechanics. The Kirsch equations [2,3,30] are:

$$\sigma_r = \frac{1}{2}(\sigma_x+\sigma_y)\left(1-\frac{R_w^2}{r^2}\right)+\frac{1}{2}(\sigma_x-\sigma_y)\left(1+3\frac{R_w^4}{r^4}-4\frac{R_w^2}{r^2}\right)\cos 2\theta+\tau_{xy}\left(1+3\frac{R_w^4}{r^4}-4\frac{R_w^2}{r^2}\right)\sin 2\theta+\frac{R_w^2}{r^2}$$

$$\sigma_\theta = \frac{1}{2}(\sigma_x+\sigma_y)\left(1+\frac{R_w^2}{r^2}\right)+\frac{1}{2}(\sigma_x-\sigma_y)\left(1+3\frac{R_w^4}{r^4}\right)\cos 2\theta+\tau_{xy}\left(1+3\frac{R_w^4}{r^4}\right)\sin 2\theta+\frac{R_w^2}{r^2}$$

$$\sigma_z = \sigma_{zz}-2\nu(\sigma_x-\sigma_y)\frac{R_w^2}{r^2}\cos 2\theta-4\nu\tau_{xy}\frac{R_w^2}{r^2}\sin 2\theta$$

$$\tau_{r\theta} = \left\{\frac{1}{2}(\sigma_x-\sigma_y)\sin 2\theta+\tau_{xy}\cos 2\theta\right\}\left(1-3\frac{R_w^4}{r^4}+2\frac{R_w^2}{r^2}\right)$$

$$\tau_{rz} = \{\tau_{xz}\cos\theta+\tau_{yz}\sin\theta\}\left(1-\frac{R_w^2}{r^2}\right) \qquad (12)$$

$$\tau_{rz} = \{-\tau_{xz}\cos\theta+\tau_{yz}\sin\theta\}\left(1+\frac{R_w^2}{r^2}\right)$$

Now there is an expression for the borehole wall or the stress state in the adjacent formation. At the borehole wall (r=a), the equations are reduced to:

Radial stress: $\sigma_r = P_w$

Tangential stress:

$$\sigma_\theta = \sigma_x+\sigma_y+P_w-2\gamma(\sigma_x-\sigma_y)\cos(2\theta)-4\tau_{xy}\sin(2\theta)$$

Axial stress, plane strain:

$$\sigma_z = \sigma_{zz}-2\gamma(\sigma_x-\sigma_y)\cos(2\theta)-4\mu\tau_{xy}\sin(2\theta)$$

Axial stress, plane stress: $\sigma_z = \sigma_{zz}$

Shear stress: $\sigma_{\theta z} = 2(\tau_{yz}\cos\theta-\tau_{yz}\sin\theta)$, $\tau_{rz} = \tau_{r\theta}$

Cartesian Stresses in three dimensions

In the petroleum industry, three principle in-situ stresses are known: the vertical or overburden stress (σ_v), and the maximum and minimum horizontal stresses (σ_H and σ_h). Since the Kirsch equations [2,3,30] supposes the horizontal, vertical, and the borehole orientation may be in any direction, these stresses should consequently be transformed into Cartesian system x, y, and z and represented as stresses σ_x, σ_y and σ_z. Equations 14 represent all transformed stress components:

$$\sigma_x = (\sigma_H\cos^2\varphi+\sigma_h\sin^2\varphi)\cos^2\gamma+\sigma_v\sin^2\gamma$$

$$\sigma_y = (\sigma_H\sin^2\varphi+\sigma_h\cos^2\varphi)$$

$$\sigma_{zz} = (\sigma_H\cos^2\varphi+\sigma_h\sin^2\varphi)\sin^2\gamma+\sigma_v\cos^2\gamma$$

$$\tau_{yz} = \frac{1}{2}(\sigma_h-\sigma_H)\sin\sin(2\varphi)\sin\gamma$$

$$\tau_{xz} = \frac{1}{2}(\sigma_H\cos^2\varphi+\sigma_h\sin^2\varphi-\sigma_v)\sin(2\gamma)$$

$$\tau_{xy} = \frac{1}{2}(\sigma_h-\sigma_H)\sin(2\varphi)\cos\gamma$$

All equations required to analyze failusres of boreholes are now defined.

Rock Failure Criteria

Formation failure criteria identify, clearly and definitely, stress conditions at failure. Common formation failure criteria as shown in Table (3) can be classified based on two main characteristics (linear or nonlinear form, and considering the effect of intermediate principal stress on the rock strength). More details and discussion are presented by Rahimi[31] and Halafawi[32].

Rock Mechanical Properties and Rock Strength Determination

The elastic moduli and the mechanical properties of a rock are basic parameters for in-situ stresses and rock strength estimation. Those are calibrated with triaxial tests in laboratory[33]. However, bulk density (ρb) values of density logs and compressional (Δt_C) and shear slowness (Δt_S) values of sonic dipole logsare utilized together in order to estimate the elastic moduli[2]:

$$\upsilon = \frac{\frac{1}{2}\left(\frac{\Delta t_s}{\Delta t_c}\right)^2-1}{\left(\frac{\Delta t_s}{\Delta t_c}\right)^2-1} \qquad (15)$$

$$G = \frac{\rho_b}{(\Delta t_s)^2} \qquad (16)$$

$$E = 2G(1+\upsilon) \qquad (17)$$

$$K = \frac{\rho_b}{(\Delta t_s)^2}-\frac{4}{3}G \qquad (18)$$

$$\lambda = K-\frac{2}{3}G \qquad (19)$$

The rock strength value which is known as the unconfined compressive strength usually termed as UCS or Co can be determined experimentally using core sample[18]. However, when core samples are not available for laboratory testing, various correlations are performed to estimate the rock value. These correlations that had been developed to predict the uniaxial compressive strength using well log data and predict the rock strength are presented by Zobak's table[18]. However, Onyia and Andrews[34] equations 20 through 21, which are based on sonic log and rock porosity, are widely used In order to estimate the rock strength at any depth because they have acceptable accuracy[34,35]. In order to reach a higher level of UCS prediction accuracy, Amani and Shahbazi[36] new correlation 23, which is employing the porosity in rock strength estimation by using sonic travel time and porosity, is used.

Citation: Halafawi DIM, Avram DIL. Wellbore instability prediction and performance analysis using Poroelastic modeling. *J Oil Gas Petrochem Sci.* (2019);2(2):93-106. DOI: 10.30881/jogps.00028

$$UCS = \frac{1}{K_1(\Delta t_c - K_2)^{K_3}} + K_4 \quad (20)$$

$$UCS = \frac{149595\left(1-\varphi^{0.18}\right)f}{(\Delta t_c - 40)^{0.42}} \quad (21)$$

$$\mathbf{UCS} = 194.4 - 0.6072\Delta\mathbf{t_c} - 646.1\boldsymbol{\varphi} - 0.01644\Delta\mathbf{t_c}^{\,2} + 8.792\boldsymbol{\varphi}\Delta\mathbf{t_c} \quad (22)$$

Where

$$f = -0.0016d^4 + 0.0181d^3 - 0.075d^2 + 0.312d + 0.5$$

K_1, K_2, K_3, and K_4 are lithology dependent Constants (Table 4)

Table 3. Common rock failure criteria

Failure Criterion Name	Failure Criterion Formula
Mohr-Coulomb	$\tau = \mu\sigma + C \quad , \quad \mu = \tan\varnothing$
Mogi-Coulomb	$\tau_{oct} = a + b\sigma_{m,2}$ $\sigma_{m,2} = \frac{1}{3}(\sigma_1+\sigma_3)$ $\tau_{oct} = \frac{1}{3}\sqrt{(\sigma_1-\sigma_2)^2+(\sigma_1-\sigma_3)^2+(\sigma_2-\sigma_3)^2}$ $a = \frac{2\sqrt{2}}{3}\frac{C_0}{q+1}, \quad b = \frac{2\sqrt{2}}{3}\frac{q-1}{q+1}$
Tresca	$\frac{(\sigma_1+\sigma_3)}{2} = C = \tau_{max}, \quad \frac{C_O}{2} = C$
Von Mises	$\sqrt{J_2} = \sqrt{\frac{(\sigma_1-\sigma_2)^2+(\sigma_1-\sigma_3)^2+(\sigma_2-\sigma_3)^2}{6}} = \frac{C_O}{3}$
Drucker-Prager	$\sqrt{J_2} = k + \alpha J_1, \quad J_1 = \frac{\sigma_1+\sigma_2+\sigma_3}{3}$
Hoek-Brown	$\sigma_1 = \sigma_3 + \sqrt{mC_0\sigma_3+sC_O^2}$
Modified Lade	$\frac{I''^3_1}{I''_3} = \eta_1 + 27$ $I''_1 = (\sigma_1+S)+(\sigma_2+S)+(\sigma_3+S)$ $I''_3 = (\sigma_1+S).(\sigma_2+S).(\sigma_3+S)$
Modified Wiebols-Cook	$\sqrt{J_2} = A + BJ_1 + CJ_1^2$
Griffith	$(\sigma_1-\sigma_3)^2 = 8T_O(\sigma_1+\sigma_3)$ $\sigma_3 = -T_O \text{ IF } (\sigma_1+3\sigma_3) < 0, \text{ and } T_O = \frac{C_O}{8}$
Modified Griffith	$\sigma_1\left[\sqrt{\mu^2+1}-\mu\right] - \sigma_3\left[\sqrt{\mu^2+1}+\mu\right] = 4T_O$ $4T_O = \frac{4}{\sqrt{\mu^2+1}-\mu}$
Murrel	$(\sigma_1-\sigma_3)^2 + (\sigma_1-\sigma_2)^2 + (\sigma_2-\sigma_3)^2 = 24T_O(\sigma_1+\sigma_2+\sigma_3)$
Stassi d'Alia	$(\sigma_1-\sigma_3)^2 + (\sigma_1-\sigma_2)^2 + (\sigma_2-\sigma_3)^2 = 2(C_o-T_o)(\sigma_1+\sigma_2+\sigma_3) + 2C_oT_o$

Citation: Halafawi DIM, Avram DIL. Wellbore instability prediction and performance analysis using Poroelastic modeling. *J Oil Gas Petrochem Sci.* (2019);2(2):93-106. DOI: 10.30881/jogps.00028

Table 4. Lithology Dependent Constants for Onyia's Equation.

Lithology	Sandstone	Shale	Combo	Limestone	Dolomite
K_1	403275	54754	74794	123913	6076
K_2	23.87	23.87	23.87	23.87	0
K_3	2.35	1.80	1.92	2	1
K_4	0	0	0	0.014	20.99

Time-Based Wellbore Stresses

The induced stresses due to the fluid flow between the wellbore and a permeable formation are presented by Detournay and Cheng[37] as shown in equations 23 through 25. In order to express the equations in time domain, a numerical Laplace inversion to the analytical solution of these equations. Stehfest method[38] is utilized for this inversion. The induced stresses solutions in time domain are expressed and derived for linear elastic rock deformation to find the fully coupled equations as shown in equations 26.

$$\Delta \mathbf{Pr}_t^{\sim} = -\left(\frac{1}{s}\right)\frac{K_o(\xi)}{K_o(\beta)} \quad (23)$$

$$\Delta\sigma_r^{\sim} = -2\eta\left(\frac{P_r}{s}\right)\left[\frac{R_w}{r}\frac{K_1(\xi)}{\beta K_o(\beta)} - \frac{R_w^2}{r}\frac{K_1(\beta)}{\beta K_o(\beta)}\right] \quad (24)$$

$$\Delta\sigma_\theta^{\sim} = 2\eta\left(\frac{P_r}{s}\right)\left[\frac{R_w}{r}\frac{K_1(\xi)}{\beta K_o(\beta)} - \frac{R_w^2}{r^2}\frac{K_1(\beta)}{\beta K_o(\beta)} + \frac{K_1(\xi)}{K_o(\beta)}\right] \quad (25)$$

Where

$$\eta = \alpha\frac{(1-\upsilon)}{2(1-\upsilon)}, \xi = r\sqrt{\frac{s}{c}}, \beta = R_w\sqrt{\frac{s}{c}}, c = \frac{k}{\mu}\left(\phi C_t\frac{\alpha^2}{\lambda+2G}\right)$$

$$\mathbf{P}_{rt} = \mathbf{P}_r + (\mathbf{P}_w - \mathbf{P}_r)\Delta\mathbf{P}(\mathbf{r},\mathbf{t})$$

$$\sigma_{rr} = \frac{\sigma_x+\sigma_y}{2}\left(1-\frac{R_w^2}{r^2}\right) + \frac{\sigma_x-\sigma_y}{2}\left(1+3\frac{R_w^4}{r^4}-4\frac{R_w^2}{r^2}\right)\cos 2\theta + \tau_{xy}\left(1+3\frac{R_w^4}{r^4}-4\frac{R_w^2}{r^2}\right)\sin 2\theta + P_w\frac{R_w^2}{r^2} + \Delta\sigma_r(r,t)$$

$$\sigma_{\theta\theta} = \frac{\sigma_x+\sigma_y}{2}\left(1-\frac{R_w^2}{r^2}\right) - \frac{\sigma_x-\sigma_y}{2}\left(1+3\frac{R_w^4}{r^4}\right)\cos 2\theta - \tau_{xy}\left(1+3\frac{R_w^4}{r^4}\right)\sin 2\theta - P_w\frac{R_w^2}{r^2} + \Delta\sigma_\theta(r,t)$$

$$\sigma_{zz} = \sigma_z - \upsilon\left[2(\sigma_x-\sigma_y)\frac{R_w^2}{r^2}\cos 2\theta + \tau_{xy}\frac{R_w^2}{r^2}\sin 2\theta\right]$$

$$\tau_{r\theta} = \frac{\sigma_x-\sigma_y}{2}\left(1+2\frac{R_w^2}{r^2}-3\frac{R_w^4}{r^4}\right)\sin 2\theta + \tau_{xy}\left(1-3\frac{R_w^4}{r^4}+2\frac{R_w^2}{r^2}\right)\cos 2\theta$$

$$\tau_{\theta z} = \left(-\tau_{xz}\sin\theta + \tau_{yz}\cos\theta\right)\left(1+\frac{R_w^2}{r^2}\right)$$

$$\tau_{rz} = \left(\tau_{xz}\cos\theta + \tau_{yz}\sin\theta\right)\left(1-\frac{R_w^2}{r^2}\right)$$

Wellbore Stability Model flow diagram

Figure 1 shows a flow diagram of the wellbore instability developed model procedures. It include four main parts: building MEM, time-based wellbore stress analysis, safe mud weight determination, and wellbore trajectory optimization.

Case Studies and Model Validation

Well RBS-91 Description

Well RBS-91 is a directional well, located within RBS-9 field in Romania. The well area is located in the central north-Eastern of a rift system margin. The main structures of this area are horsts, grabens, and faults striking NW-SE. This basin is described a highly active tectonic area, which lead to a high anisotropy in the horizontal stresses. The dataset of the well logs that have been recorded during the drilling phase of the well, includes cross dipole sonic log, neutron porosity log, density log and 6-arm caliper log as shown in Figures (2&3). After examining these logs, it is clearly observed that there are severe breakouts in the 8½ inch hole section as appeared in Figure (3).

Developed Model Analysis for Well RBS-91

In order to perform an excellent analysis and validate the developed model, the MEM is firstly developed for instability zones (3650 m – 3800 m) of well RBS-91 as illustrated in the preceded flow diagram. The MEM results for wellbore instability zone which include overburden stress (σv), minimum horizontal stress (σh), maximum horizontal stress (σh), bulk modulus (K), shear modulus (G), Young's modulus (E), Poisson's ratio (υ),pore pressure (Pp), and uniaxial compressive strength (UCS) are shown in Figure (4). The developed model shows that the maximum shear stress around the wellbore is at 63° and 243° counterclockwise for a long time period (30 hrs) after drilling this zone (Figure 5). The shear stress curves at different times are overlaid and reached the maximum value instantaneously at the wellbore wall (r/rw=1) for all time periods. However, the alteration of hoop stress and the time dependency are significantly realized when the radial distance (r) increases more than (rw). The shear stress curves at various times periods become separated and the effect of time appears (Figure 6). Additionally, Figure (7) shows the shear stress alteration for 4 time periods versus the radial distance from the wellbore at θ=63°. It's clearly observed that the shear stress has a maximum constant value at the wellbore wall, a significant difference around borehole wall, and becomes identical far away from wellbore wall. That means the stress magnitude decreases as the radial distance from the wellbore increases, until it reaches the value of the in-situ maximum horizontal stress. Obviously, the shear stresses increase with time and may extend the shear failure if it goes beyond the value of the rock strength. However, the failure will never be initiated with time as it is mentioned above that the shear stress value has reached at the wellbore wall instantaneously to its maximum after drilling the formation.

The developed model also shows radial stress variations with the radial distance from the wellbore for the same time periods (Figure 8).

Citation: Halafawi DIM, Avram DIL. Wellbore instability prediction and performance analysis using Poroelastic modeling. *J Oil Gas Petrochem Sci.* (2019);2(2):93-106. DOI: 10.30881/jogps.00028

The radial stress is identical to the wellbore pressure at the wellbore walls. Moving far from the wellbore, the radial stress starts to increase until it reaches the minimum in-situ horizontal stress. Moreover, Figure (9) shows pore pressure changes with respect to time and radial distance. The pore pressure is the same as the wellbore pressure once the formation is opened at the wellbore wall. Since the wellbore pressure is higher than the pore pressure (overbalance drilling), the drilling fluid invades the formation and the formation pressure starts to increase with time.

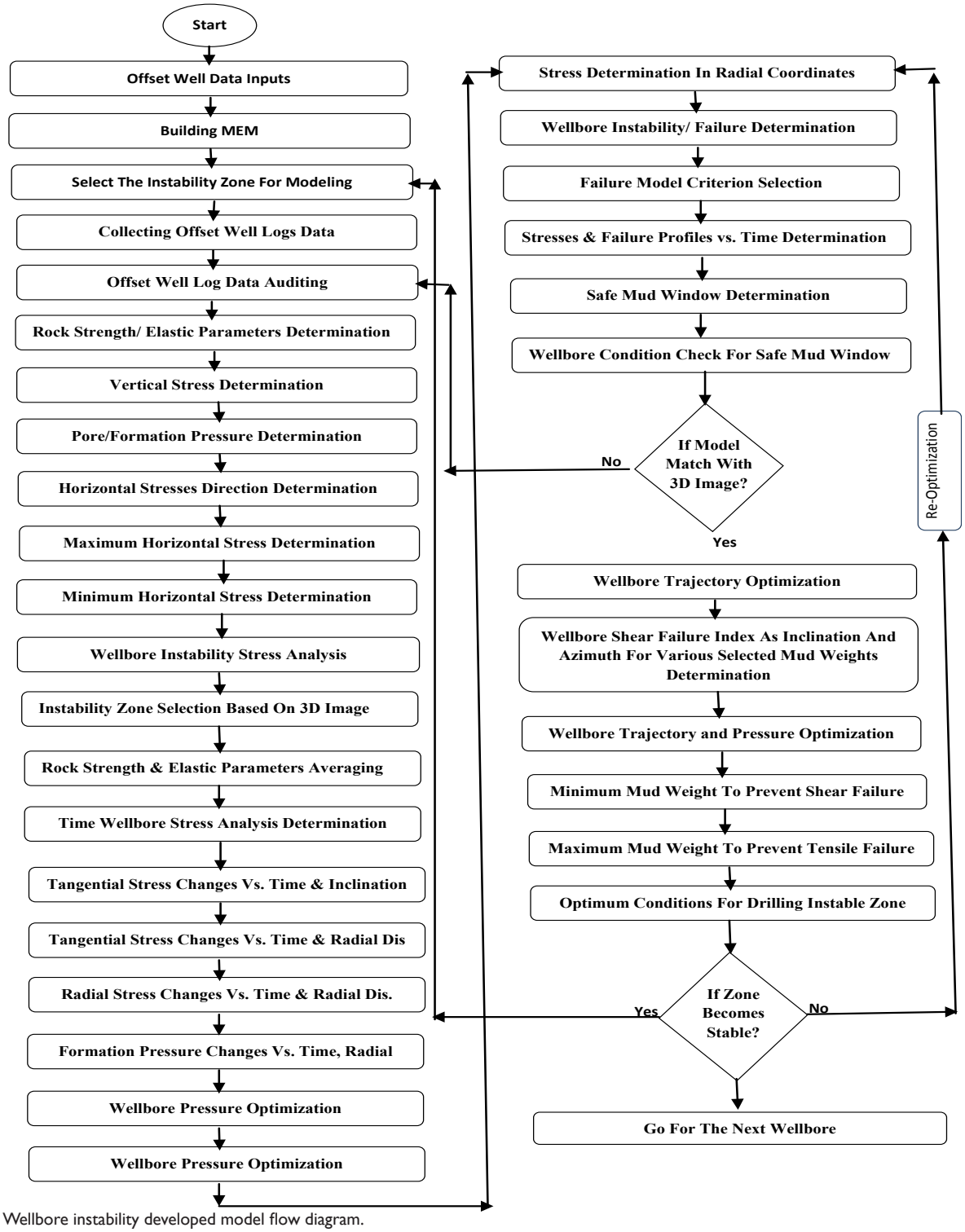

Figure 1: Wellbore instability developed model flow diagram.

Citation: Halafawi DIM, Avram DIL. Wellbore instability prediction and performance analysis using Poroelastic modeling. *J Oil Gas Petrochem Sci.* (2019);2(2):93-106. DOI: 10.30881/jogps.00028

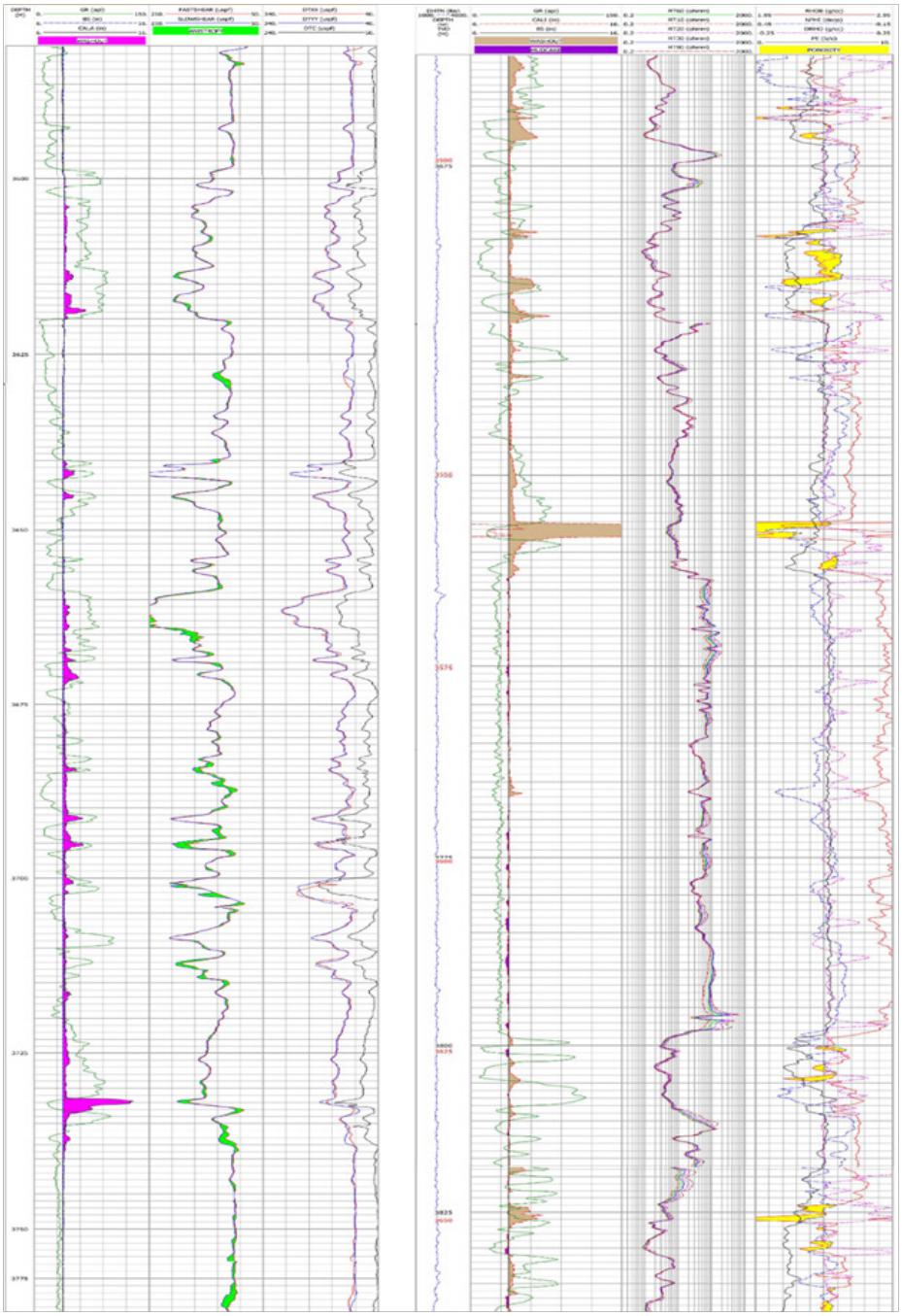

Figure 2: Composite log for well RBS-91.

In order to validate the effectiveness of the developed model, the actual mud weight, azimuth, and inclination for instability zones (3650 m – 3800 m) are utilized. The developed model results for actual and calculated ones are compared together. The model shows the radial and the shear stresses as well as the failure and the pore pressure profiles (rows) at various time periods (columns) for instability zones (Figure 10). The first row represents the radial stresses, the second is the shear stresses, the third is the failure profile and the last row is the pore pressure profile. Obviously, the propagation of shear failure is changed with time. Additionally, Figure 10 is a contour representation for shear failure index (Isf) - predicting failure obviously reduces itself to comparing the internal stresses (s) to the material's strength in the loading direction- around the wellbore at time periods 0, 1, 15, and 60 minutes. This figure is a perfect representation of the Isf which can predict the shape and the size of the shear failure of the wellbore. The blue area represents Isf < 0 hence, shear failure will take place, while the yellow area and the yellow shade represents area represents Isf > 0, hence, no shear failure. According to the developed model, a minor shear failure that will take place onset drilling is predicted. However, after 60 minutes, the model predicts that the shear failure will extend as shown in Figure 10. Comparing this result with the actual wellbore image log (Figure 3), a good match between the caliper log and failure prediction done by the developed model is observed and achieved. Therefore, the developed model has higher accuracy than the linear elastic model.

Citation: Halafawi DIM, Avram DIL. Wellbore instability prediction and performance analysis using Poroelastic modeling. *J Oil Gas Petrochem Sci.* (2019);2(2):93-106. DOI: 10.30881/jogps.00028

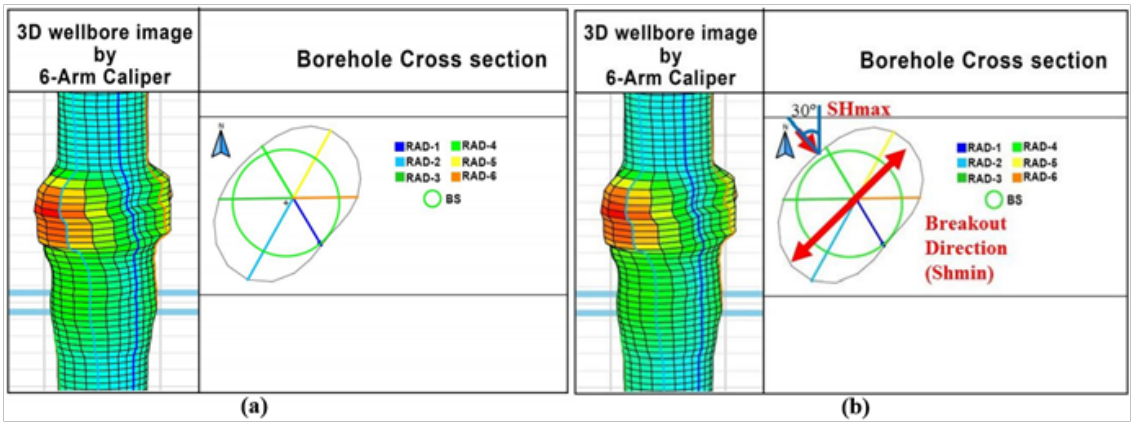

Figure 3: (a) 3D wellbore image and cross section for well RBS-91, instability zone using6-arm caliper log (b). Determination of σ_{hmax} using breakout analysis for instability zone.

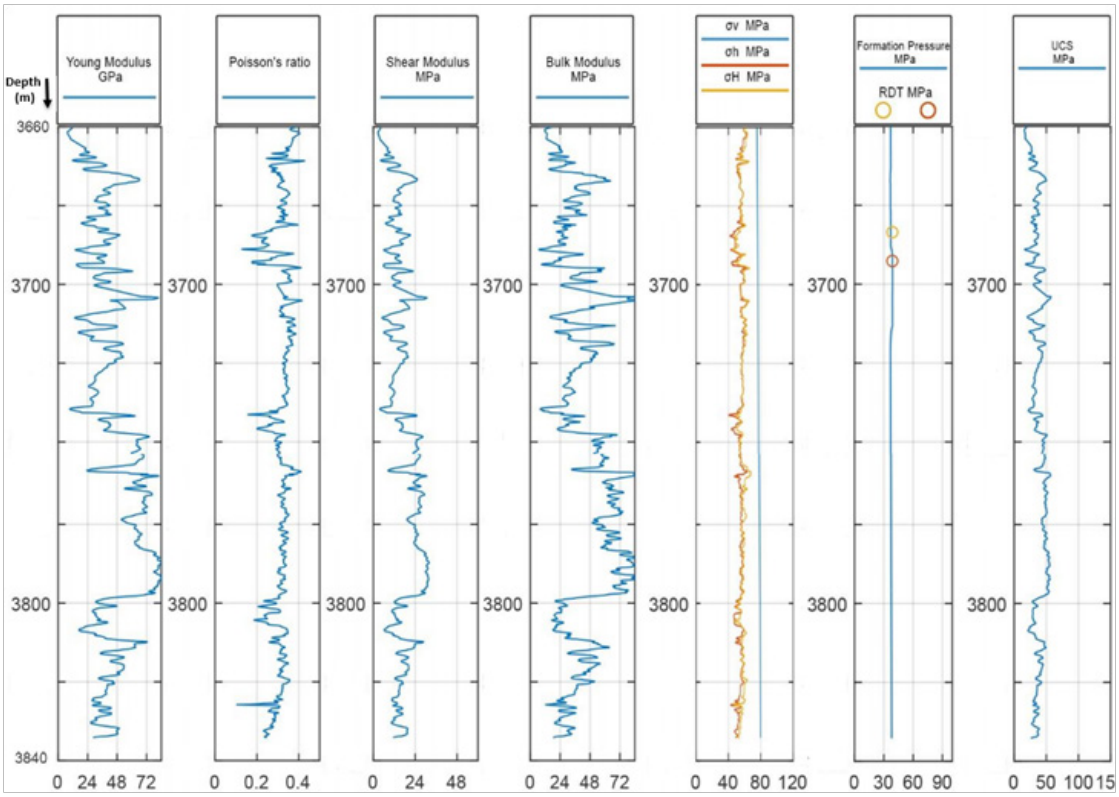

Figure 4: The MEM resultsof developed model for Well RBS-91.

The safe mud pressure window as a function of the wellbore inclination angle is predicted with the modified Lade failure criterion which is selected because it is the most common and accurate criterion in petroleum industry based on the published studies (Figure11). The red color represents a fracture region, the green color shows a safe region and the blue color indicates a collapse region. The bright color star represents the RBS-91 wellbore conditions (inclination, borehole pressure) which is located inside the collapse region. In Figure 11, it is observed that the safe pressure window is very narrow at the high deviation angle at the current well azimuth (240º). In order to resolve this failure, the mud weight should, therefore, be increased or the well inclination should be changed. As in Figure 11, if the well inclination is selected to be changed, the wellbore mud density will also vary in order to keep the well in safe window during drilling this unstable zone in future developments.

In order to remedial and mitigate the breakout failure problem associated with instability zones in the future wells, the following suggestions are recommended for remedial:

a. Optimize the borehole pressure (Increase the mud weight)

b. Optimize the wellbore trajectory (Adjust the azimuth and the inclination)

c. Optimize both of borehole pressure and trajectory

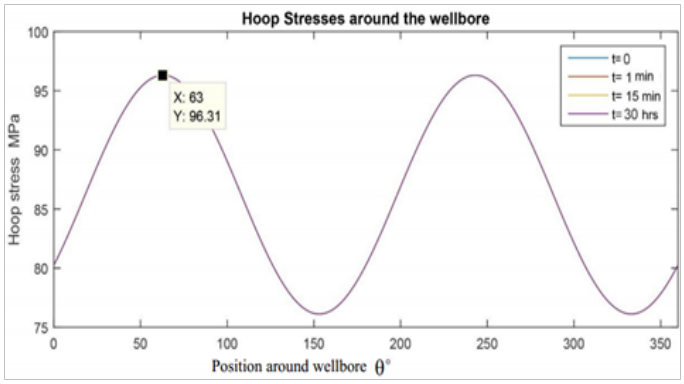

Figure 5: The poroelastic model tangential stresses as a function of inclination and time at r/R_w=1.

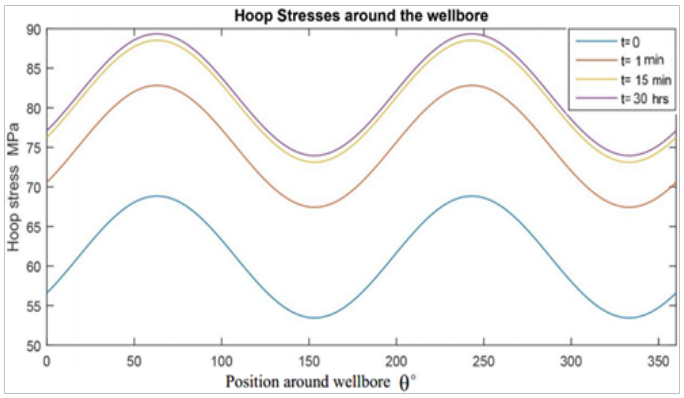

Figure 6: The poroelastic model tangential stresses as a function of inclination and time at r/R_w=1.1.

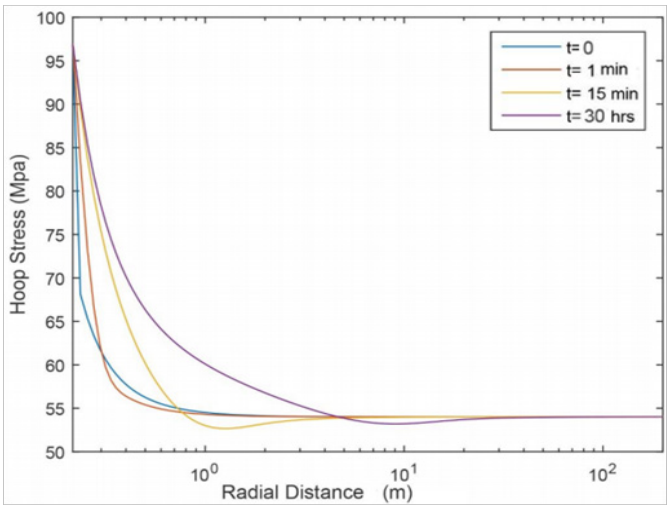

Figure 7: The poroelastic model tangential stresses as a function of radial distance and time.

For wellbore pressure optimization, the developed model optimizes the mud weight required to tackle instability problem using the most common failure criterion in petroleum industry (Modified Lade). It shows that the minimum and maximum safe mud weight in order to avoid shear and tensile failure are 9.8 and 15.5 ppg respectively (Figure 12). This is because 9.8 and 15.5 ppg represent the minimum and the maximum safe curves for instability zone. However, the wellbore trajectory optimization is shown in Figure 13 a through d in which a stereo net map is representing the shear failure index (Isf) as a function of wellbore azimuth and inclination. The color map of the plot indicates how far the well is away from the shear failure, blue is the safest region, and red is a failure region. The actual wellbore trajectory is represented with the black circle on the map. Obviously, the wellbore stability cannot be maintain with the current mud weight for any well trajectory, therefore the wellbore trajectory optimization is not enough to avoid the wellbore failure. As a result, this solution is not applicable. Changing the mud weight with alternating wellbore inclination and azimuth would result in selecting the optimum trajectory. The more the mud weight, the safer wellbore trajectory is shown and the more easy to drill this section without collapse failure using different wellbore trajectories (Figure13). However, there is a limit for increasing the mud weight to avoid fracture the formation. Therefore, the optimum wellbore trajectory that can be drilled safely utilizing the minimum mud weight should be determined. Optimization of borehole pressure and well trajectory is then required. The minimum required mud weight to prevent shear failure and the maximum required mud weight to avoid tensile failure as a function of wellbore azimuth and deviation angles are presented in Figure (13e&f). As an overview on the relationship between the wellbore trajectory and the optimum mud weight, this well section obviously cannot be drilled horizontally in direction of the minimum horizontal stress (Azimuth = 60º) due to the narrow allowable mud window.

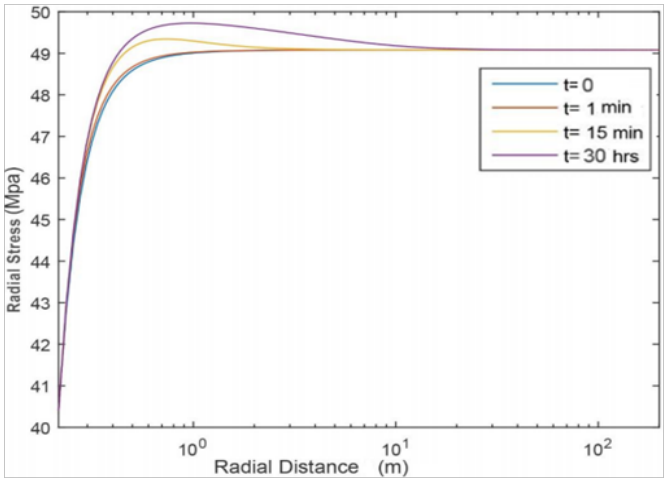

Figure 8: The poroelastic model radial stresses as a function of radial distance and time.

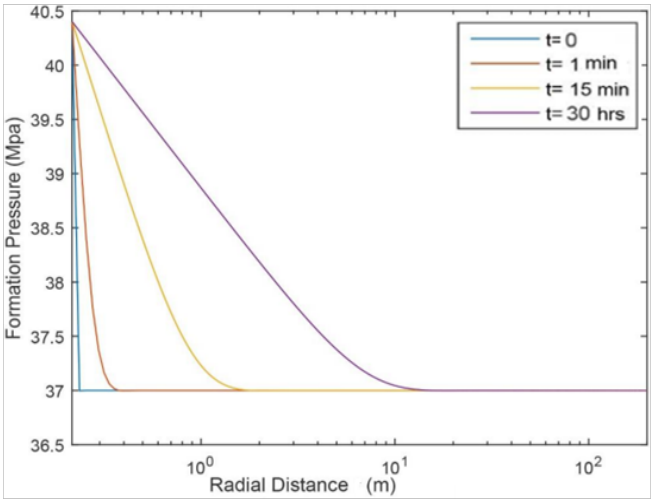

Figure 9: The poroelastic model pore pressure as a function of radial distance and time.

Citation: Halafawi DIM, Avram DIL. Wellbore instability prediction and performance analysis using Poroelastic modeling. *J Oil Gas Petrochem Sci.* (2019);2(2):93-106. DOI: 10.30881/jogps.00028

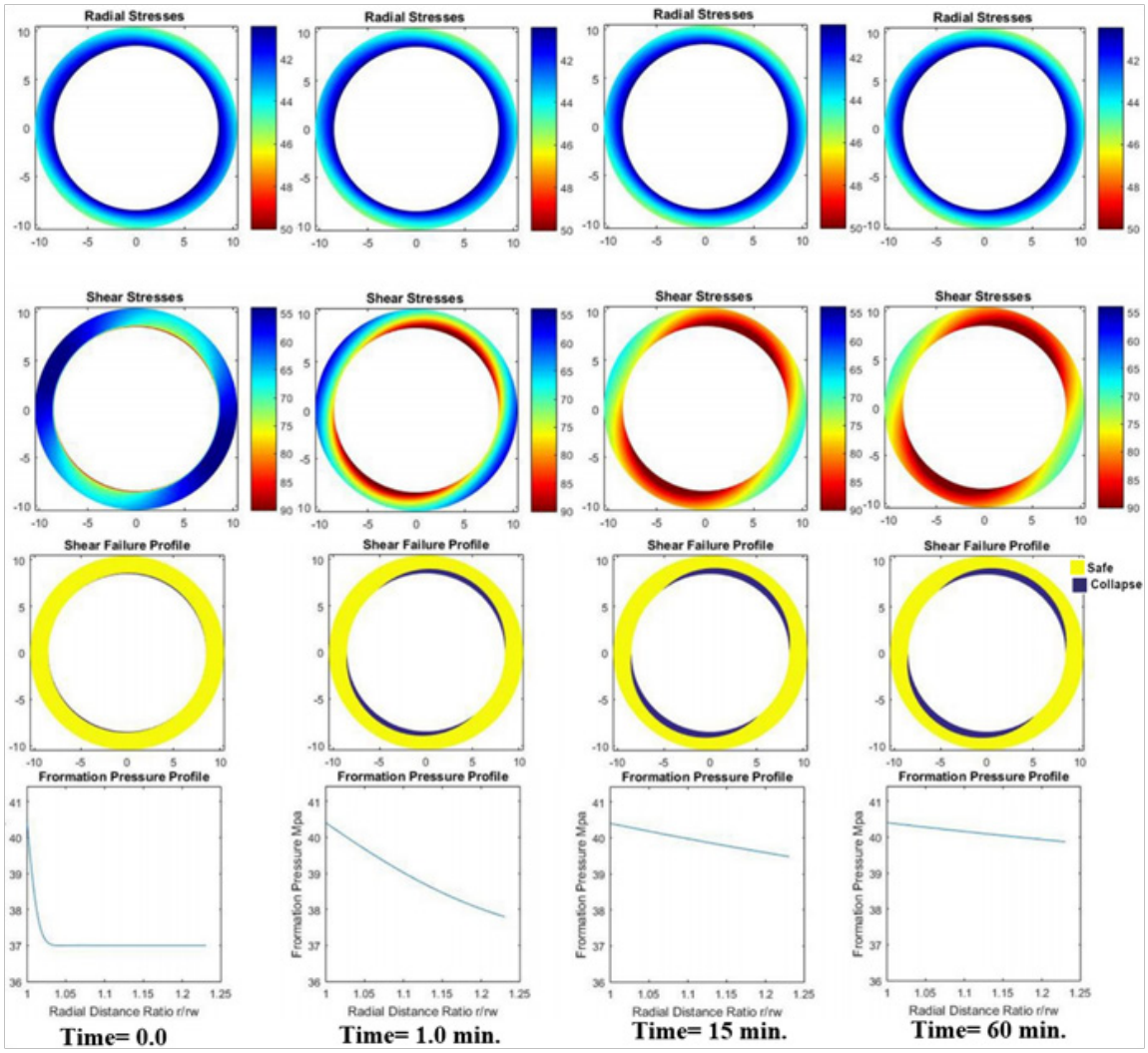

Figure10: Stresses and failure profiles as a function of time for instability zones.

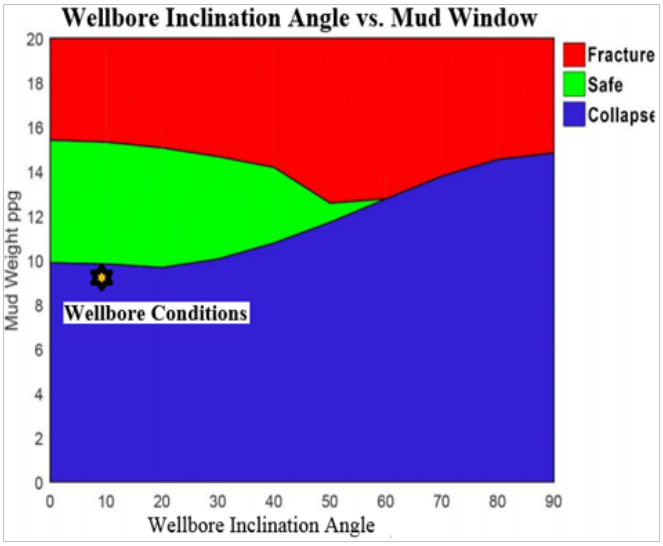

Figure 11: Mud pressure window function of inclination angle for instability zones.

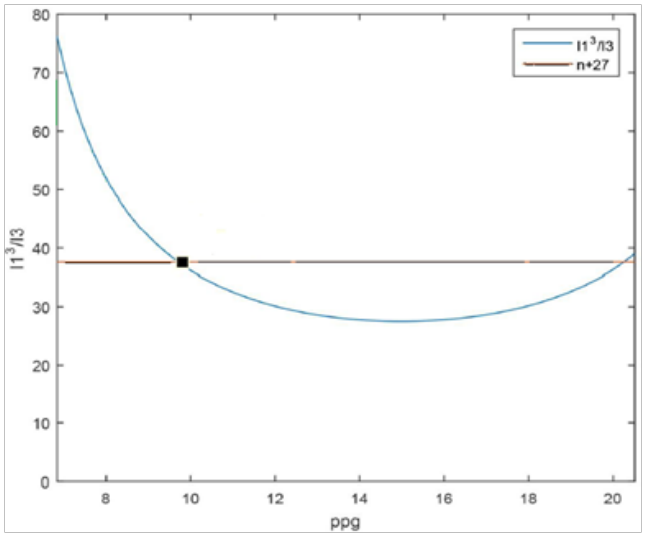

Figure 12: Modified Lade criterion function of wellbore pressure for Instability zone.

Citation: Halafawi DIM, Avram DIL. Wellbore instability prediction and performance analysis using Poroelastic modeling. *J Oil Gas Petrochem Sci.* (2019);2(2):93-106. DOI: 10.30881/jogps.00028

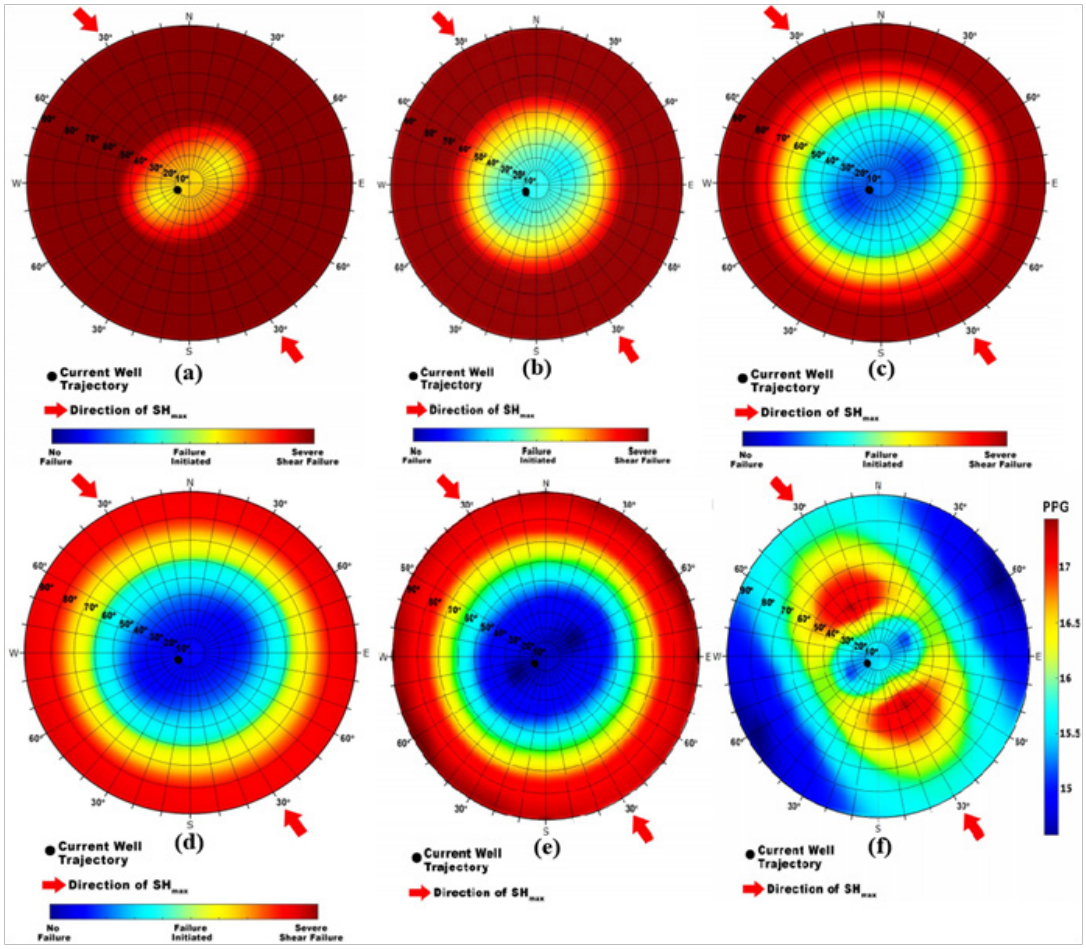

Figure13: (a, b, c, d) The model shear failure index projection on Stereo net map function of inclination and azimuth Mwt 9.2 ppg, 10.2 ppg, 11.2 ppg, and 12.2 pp respectively.(e, f)Minimum and maximum allowable mud weight as function of well inclination and azimuth respectively.

Conclusions and Recommendations

A time-dependent developed model for wellbore instability prediction was implemented in this article. The developed model is effectively predicting the safe mud weight window and optimizing the wellbore trajectory. Based on the results and analysis, the following conclusions and recommendations are extracted:

1. Well bore instability are predicted utilizing available well log and drilling data without available core measurements.
2. The developed model is successful for predicting instability zones
3. The failure criteria with the effect of intermediate principal stress show an effective way for rock failure description in the developed model more than those which are not considered the intermediate principal stress.
4. The poroelastic model yielded better accuracy to predicting wellbore failure with time.
5. The mitigation of wellbore instability can be performed by increasing the mud weight or orienting the wellbore to different direction. However, in some cases, the change in wellbore trajectory is not enough and mud weight must be increased.
6. The developed wellbore instability model is potentially applicable to other field cases using a similar approach which could be adjusted to the particular field specifications and requirements.

Nomenclatures

a_s, b_s = *Rock coefficient values*

c = *generalized consolidation coefficient (Diffusion coefficient)*

C_o = *Unconfined compressive strength of rock (Uniaxial Compressive strength),*

C'_2, C'_1 =*Constants calculated by the rock properties at the test depth*

c_t = *rock total compressibility which is equal to the inverse of the Bulk modulus of elasticity K.*

d = *depth in km*

E = *Young's modulus*

G = *Shear modulus*

g = *gravitational acceleration.*

h = *depth, ft.*

k = *absolute permeability*

Citation: Halafawi DIM, Avram DIL. Wellbore instability prediction and performance analysis using Poroelastic modeling. *J Oil Gas Petrochem Sci.* (2019);2(2):93-106. DOI: 10.30881/jogps.00028

K= Bulk Modulus

K_0, K_1 = zero and the first order of modified Bessel function of the second kind

P_e=Pressure difference between minimum horizontal stress and pore pressure of formation.

P_p= Pore pressure, psi

Pr= pore pressure,

Prn =normal pore pressure which equivalent to vertical height of a column of water along from the surface to the formation of interest

S_h=Minimum horizontal stress from the test data,

r= position radially outwards from the center

R_w, r =Wellbore radius and the radius of investigation

x = an exponent

α_b= Biot Coefficient

β = Angle of fault plan, degrees=$\pi/4 - \phi/2$

γ = the borehole inclination from vertical, degrees

Δt_c = sonic compressional travel time in µsec/m

Δt_{log}= observed acoustic travel time from the sonic log

Δt_{norm} = normal acoustic travel time

λ = Lame's Parameter

μ = fluid viscosity

(h) = the density of the rock at depth (h)

ρ_b= Bulk density for rock, lb/ft.^{3}

σ_{tec}=Additional tectonic stress

σ_v= Overburden stress, psi

σ_H= Maximum horizontal stress, psi

σ_h= Minimum horizontal stress, psi

υ= Poisson's ratio

θ= angle with the direction of the maximum horizontal stress

ϕ= porosity of rock, fraction

$\varnothing$ = Internal friction angle

φ=the geographical azimuth and the borehole position from the x-axis, θ.

υ_{slow}, υ_{fast} =Poisson's ratios using the slow shear and fast shear travel time respectively.

S_1=Parameters of failure criterion function of the cohesion of the rock (Co) and internal friction angle ($\varnothing$)

η = poroelastic coefficient

References

1. Azar JJ, G Robello Samuel. Drilling Engineering. PennWell Corporation, published book, USA. 2007.
2. Fjaer E, Holt R, Raaen AM, et al. Petroleum Related Rock Mechanics, second edition. Developments in Petroleum Science,53. Amsterdam: Elsevier Science Publishers. 2008.
3. Bernt Aadnoy, Reza Looyeh. Petroleum Rock Mechanics. Drilling Operations and Well Design, Gulf Professional Publishing is an imprint of Elsevier, USA, 2011.
4. Robert FM, Stefan ZM. ''Fundamentals of Drilling Engineering'', SPE, 2011.
5. Fjær E, Holt RM, Horsrud P, et al. Petroleum related rock mechanics. 1992.
6. Fuh GF, EG Dew, CA Ramsey, et al. "Borehole-Stability Analysis for the Design of the First Horizontal Well Drilled in the U.K. Southern V Fields," SPE Drilling Engineering. 1991;6(3):169–176 ·
7. Ong SH, Roegiers JC. Horizontal wellbore collapse in an anisotropic formation. In: Paper SPE 25504. Presented at SPE Production Operations Symposium, 21-23 March, Oklahoma City, Oklahoma. 1993.
8. Morita N. "Well Orientation Effect on Borehole Stability," SPE Annual Technical Conference and Exhibition, 26-29 September, Houston, Texas, 2004.
9. Hodge MO, Valencia KJL, Z Chen, et al. "Analysis of Time-Dependent Wellbore Stability of Underbalanced Wells Using a Fully Coupled Poroelastic Model," SPE Annual Technical Conference and Exhibition, 24-27 September, San Antonio, Texas, USA, 2006.
10. Rabaa AS, HH Abass, DE Hembling, et al. "A Geomechanical Facies-Based Approach To Optimize Drilling and Completion Strategy of an Unconsolidated Sandstone Reservoir, Saudi Arabia," SPE Annual Technical Conference and Exhibition, 11-14 November, Anaheim, California, USA, 2007.
11. Li S, CC Purdy. "Maximum Horizontal Stress and Wellbore Stability While Drilling: Modeling and Case Study," SPE Latin American and Caribbean Petroleum Engineering Conference, 1-3 December, Lima, Peru, 2010.
12. Qi Z, Nawrocki PA, D Wang. "Modeling Poroelastic Effect on Borehole Stability for Under-balanced and Over-balanced Drilling Conditions," ISRM Regional Symposium - 7th Asian Rock Mechanics Symposium, 15-19 October, Seoul, Korea, 2012.
13. Manshad AK, Jalalifar H, Aslannejad M. Analysis of vertical, horizontal and deviated wellbores stability by analytical and numerical methods. *Journal of Petroleum Exploration and Production Technology*. 2014;4(4):359–369.
14. Halafawi M, Avram L. Wellbore trajectory optimization for horizontal wells: the plan versus the reality. *J Oil Gas Petrochem Sci*. 2019;2(1):49–54.
15. Yi X, Goodman HE, Williams RS, et al. Building a geomechanicalmodel for Kotabatak field with applications to sanding onset and wellbore stability predictions. In: IADC/SPE Asia Pacific Drilling Technology Conference and Exhibition. Society of Petroleum Engineers, 2008.
16. Mohiuddin MA, Khan K, Abdulraheem A, et al. Analysis of wellbore instability in vertical, directional, and horizontal wells using field data. *Journal of Petroleum Science and Engineering*. 2007;55(1-2):83–92.
17. Chabook M, Al-Ajmi A, Isaev V. The role of rock strength criteria in wellbore stability and trajectory optimization. *International Journal of Rock Mechanics and Mining Sciences*. 2015;(80):373–378.
18. Zobak MD. Reservoir Geomechanics. United Kingdom: Cambridge University Press, 2007.
19. Hudson JA, JP Harrison. Engineering Rock Mechanics-An Introduction to the Principles Amsterdam, Lausanne, New York, Oxford, Shannon, Singapore, Tokyo: Pergamon, 1997.

20. Biot MA, Willis DG. "The Elastic Coefficient of the Theory of Consolidation,". *Journal of Applied Mechanics*. 1957;24: 594–618.
21. Ahmed U, Markley ME, Crary SF. "Enhanced In-Situ Stress Profiling With Micro fracture, Core, and Sonic-Logging Data," SPE Journal, 1991.
22. Cipolla CL, Liu D, Kyte DG. "Practical Application of In-Situ Stress Profiles," SPE Annual Technical Conference and Exhibition, 25-28 September, New Orleans, Louisiana, 1994.
23. Iverson WP. "Log-derived Stress In Anisotropic Formations," Society of Petro physicists and Well-Log Analysts, 1996.
24. Blanton TL, Olson JE. "Stress Magnitudes from Logs: Effects of Tectonic Strains and Temperature," SPE Journal, 1999.
25. Hari Krishnan R, Hare land G. "Prediction of Minimum Principal In-Situ Stress by Comparison and Verification of Four Methods, "SPE Asia Pacific Oil and Gas Conference, 20-22 March, Kuala Lumpur, Malaysia, 1995.
26. Addis MA, Last NC, Yassir NA. "Estimation of Horizontal Stresses at Depth in Faulted Regions and Their Relationship to Pore Pressure Variations," SPE Journal, 1996.
27. Barton CA, Zoback MD, Burns KL. "In-situ stress orientation and magnitude at the Fenton Geothermal Site, New Mexico, determined from well bore break outs," Geophysical Research Letters, 1988;15: 467–470.
28. Crain, P Eng Crain's Petro physical Handbook. Sonic Travel Time (Slowness) Logs, 2013.
29. Eaton BA. "The Equation for Geo pressure Prediction from Well Logs," Fall Meeting of the Society of Petroleum Engineers of AIME, 28 September-1 October, Dallas, Texas, 1975.
30. Aadnoy BS. (1997, rev 2003), An introduction to petroleum rock mechanics, compendium, University of Stavanger.
31. Rahimi R, Nygaard R. " What Difference Does Selection of Failure Criteria Make in Wellbore Stability Analysis?" ARMA 14-7146, 48th US Rock Mechanics/Geomechanics Symposium held in Minneapolis, MN, USA. 2014;1–4.
32. Halafawi M, Avram L. "Borehole In situ Stress Stability Analysis of RBS-9 Field Utilizing the Inversion Technique," Journal of Engineering Sciences and Innovation, Petro leumand Mining Engineering Section (F), 2019;4(1).
33. Bozorgi E, Javani D, Rastegarnia M. "Development of a mechanical earth model in an Iranian off-shore gas field". *Journal of Mining and Environment*. 2016;7:37–46.
34. Andrews RJ, Hareland G, Nygaard R, et al. "Methods of Using Logs to Quantify Drillability," Rocky Mountain Oil & Gas Technology Symposium, 16-18 April, Denver, Colorado, USA, 2007.
35. Onyia EC. "Relationships Between Formation Strength, Drilling Strength, and Electric Log Properties," SPE Annual Technical Conference and Exhibition, 2-5 October, Houston, Texas. 1988.
36. Amani A, Shahbazi K. "Prediction of Rock Strength using Drilling Data and Sonic Logs." *International Journal of Computer Applications*. 2013;81.
37. Detournay E, Cheng AHD. "Poroelastic response of a borehole in a non-hydrostatic stress field." *International Journal of Rock Mechanics and Mining Sciences & Geomechanics Abstracts*. 1988;25:171–182.
38. Stehfest H. "Algorithm 368: Numerical inversion of Laplace transforms [D5]," Commun. ACM. 1970;13:47–4 9.